Distribution Agreement

In presenting this thesis or dissertation as a partial fulfillment of the requirements for an advanced degree from Emory University, I hereby grant to Emory University and its agents the non-exclusive license to archive, make accessible, and display my thesis or dissertation in whole or in part in all forms of media, now or hereafter known, including display on the world wide web. I understand that I may select some access restrictions as part of the online submission of this thesis or dissertation. I retain all ownership rights to the copyright of the thesis or dissertation. I also retain the right to use in future works (such as articles or books) all or part of this thesis or dissertation.

Signature:

_____ _____

Michelle Leidy Date

Developing Redox-Active Ligands That Incorporate Intramolecular Hydrogen Bonding: Novel Reactivity of High-Spin Co(II) Complexes

By

Michelle R. Leidy
Master of Science

Chemistry

_____
Cora E. MacBeth, Ph. D.
Advisor

_____
Huw M. L. Davies, Ph. D.
Committee Member

_____
Nathan T. Jui, Ph. D.
Committee Member

Accepted:

_____
Lisa A. Tedesco, Ph.D.
Dean of the James T. Laney School of Graduate Studies

_____
Date

Developing Redox-Active Ligands That Incorporate Intramolecular Hydrogen Bonding: Novel Reactivity of High-Spin Co(II) Complexes

By

Michelle R. Leidy
B. S., Sewanee: The University of the South, 2015

Advisor: Cora E. MacBeth, Ph. D.

An abstract of A thesis submitted to the Faculty of the James T. Laney School of Graduate Studies of Emory University in partial fulfillment of the requirements for the degree of Master of Science in Chemistry

2018

Abstract

Developing Redox-Active Ligands That Incorporate Intramolecular Hydrogen Bonding: Novel Reactivity of High-Spin Co(II) Complexes

By Michelle R. Leidy

Redox-active ligands have the potential to allow inexpensive and environmentally benign 1st row transition metals to mimic 2nd and 3rd row transition metal chemistry, as well as provide opportunities to explore new chemistry. Our research group has been developing catalysts for O-atom transfer, C-H amination, and aerobic deformylation using high-spin Co^{II} ions supported by a redox-active NNN-pincer ligand. A new variant of this parent catalyst, H_5L^{Urea}, has been synthesized that incorporates hydrogen-bond donating groups into this pincer ligand in order to modulate reactivity. The hydrogen-bond donors are expected to help stabilize higher oxidation states and negatively charged exogenous ligands. The H_5L^{Urea} ligand and its subsequent Co^{II} complex can be synthesized and can be studied using a variety of methods. Exogenous ligands, such as O_2, were added to the complex to see if they would bind, and if they did, what kind of reactivity they would have compared to its non-H-bonding analogue. Upon addition of O_2, it formed a highly oxidized, five-coordinate species, which differs drastically compared to the previously reported complex that instead activated the O_2. This reaction has been monitored using absorbtion spectroscopy, and the product was crystallized and characterized by X-ray crystallography, NMR, and IR. The effect of H-bonding in the ligand of this Co^{II} complex is demonstrated by its difference in O_2 reactivity. The five-coordinate species is a new and unusual finding, which may help achieve more challenging oxidations in the future.

Developing Redox-Active Ligands That Incorporate Intramolecular Hydrogen Bonding: Novel Reactivity of High-Spin Co(II) Complexes

By

Michelle R. Leidy
B. S., Sewanee: The University of the South, 2015

Advisor: Cora E. MacBeth, Ph. D.

A thesis submitted to the Faculty of the James T. Laney School of Graduate Studies of Emory University in partial fulfillment of the requirements for the degree of Master of Science in Chemistry

2018

Table of Contents

List of Figures

List of Schemes

List of Tables

Chapter 1 General Introduction

Redox-Active Ligands

A large portion of catalysis relies on 2-electron transformations that can be easily provided by noble metals, such as Rh, Ir, and Pt, which are scarce and costly[1]. Less expensive, more earth-abundant metals can help synthesis become more sustainable and cost-efficient, but only if they can outcompete their 2nd and 3rd row counterparts. 2nd and 3rd row transition metals are proficient at multi-electron chemistry. However, since 1st row transition metals are predominantly known for their 1-electron processes, the extra electrons to carry out these multi-electron transformations must come from somewhere else. One viable option to overcome this obstacle is to use "redox-active" or "redox non-innocent" ligands, which can participate in the redox processes that are a part of the catalytic cycle and play a more pronounced role in bond activation[2]. These ligands can be the key to allowing 1st row transition metals mimic their 2nd and 3rd row counterparts.

Redox active ligands have been known to exist in multiple oxidation states while coordinated to a metal center. The orbitals of the ligands are spatial and energetic proximity to the metal d-orbitals and lead to mixing, often making it hard to assign formal oxidation states[3]. This concept has been studied since the 1960s. In the example shown in Figure 1.1, Schrauzer and Mayweg synthesized the neutral dithiolene nickel complex and speculated that two electrons had to reside in low-lying ligand orbitals, otherwise the metal center would have to be Ni(0). They found that their magnetic measurements did correspond to a Ni(II) center[4]. Gray and Billig then synthesized similar Pd(II), Pt(II), Co(II), Cu(II), and dithiolene complexes that exhibited the same electronic properties and identical square planar geometries[5]. In addition, Davison, *et. al.* prepared the neutral metal dithiolene complexes and used a series of electron transfer reactions to make the mono- and dianionic

analogues. Their EPR, magnetic, and electrochemical results all pointed to the ligand backbone being oxidixed and reduced while retaining the M(II) center[6]. This showed that redox-active ligands could work in tandem with 1st row transition metals, providing the extra electron(s) to facilitate multi-electron processes that the metal otherwise would not be able to do.

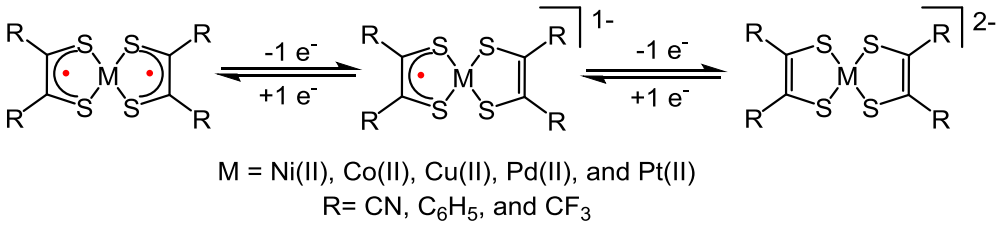

Figure 1.1. From left to right: neutral, monoanionic, and dianionic dithiolene metal complexes

Redox-active ligands can influence the reactivity of a catalyst in several ways. One way is through the modification of Lewis acidity of the metal. In non-redox active ligands, this is accomplished by incorporating electron-donating or -withdrawing groups into the ligand, which usually requires separate ligand synthesis and potentially a change in steric environment. With redox-active ligands, one only needs to change the oxidation state of the ligand to influence the metal's Lewis acidity. This easily changes the catalyst's affinity for certain substrates over others.

The concept of tuning the Lewis acidity is easily seen in the works of Ruachfuss, *et. al.*[7] and Wrighton, *et. al.*[8] In the former case, for the oxidation of H_2, the catalyst's metal center is more acidic once the ligand is oxidized to form a cationic species (Scheme 1.1). This allows it to react with dihydrogen to form the H_2 adduct, which is in turn deprotonated by a non-coordinating base. The extra electrons end up reducing the ligand to its neutral form, so in this case the ligand also serves as an electron reservoir. In the latter case, increasing the basicity helps facilitate the rate determining step (oxidative addition) of the

hydrogenation of olefins. With their cobaltacene ligand moiety, both mono- and dicationic complexes are active, but the reduced form is 16 times faster. It was speculated that the oxidative addition of the H_2 was promoted by more electron-rich metal centers.

Scheme 1.1. Ligand Oxidation Leading to Increased Lewis Acidity of the Metal

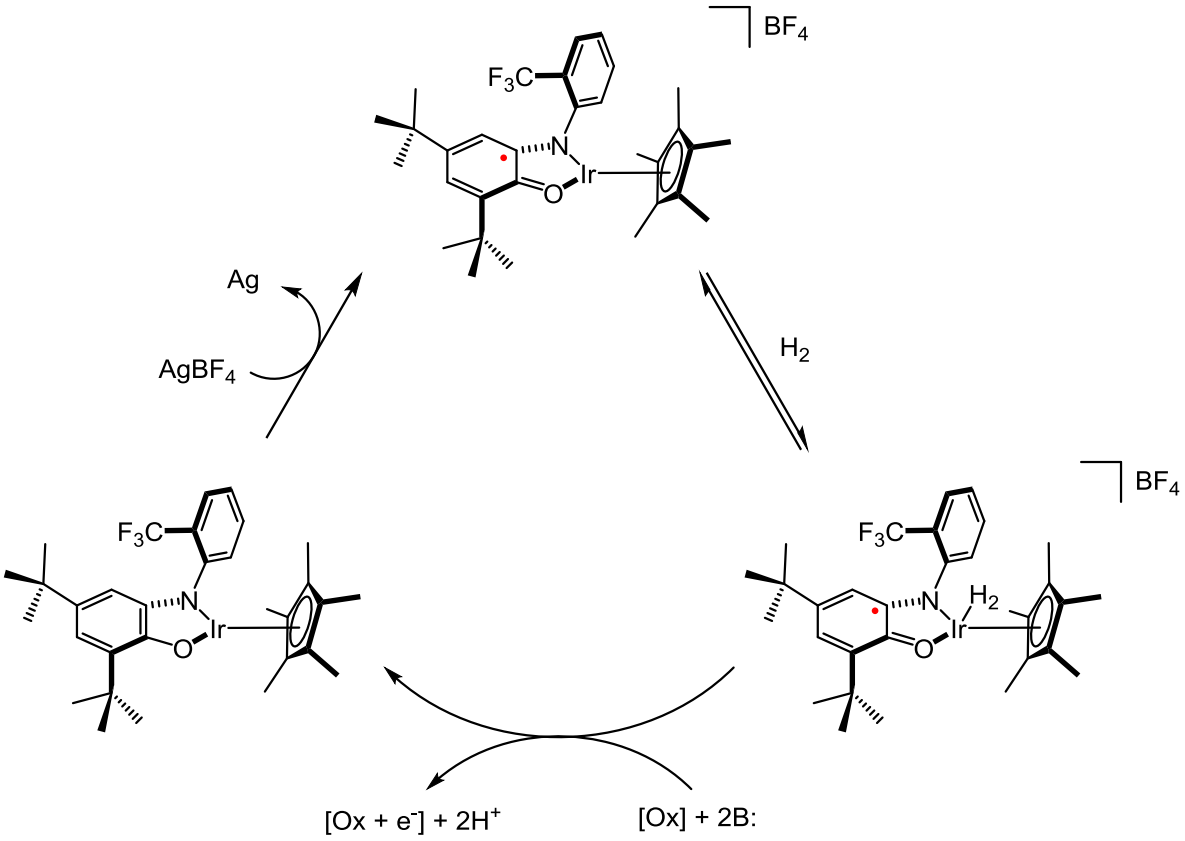

Another way these ligands shape reactivity is by serving as "electron reservoirs," meaning that electron density can be stored in the ligand framework in order to avoid unfavorable or uncommon metal oxidation states. It is in this way that 1st row transition metals can directly parallel the 2nd and 3rd row metals. Oxidative addition and reductive elimination are both 2-electron processes within many catalytic cycles, and is not usually a problem for noble metal catalysts[2]. For the 1st row metal complexes, if they contain redox-active ligands, one or both of the electrons needed for those steps can be stored or taken from the ligand, leaving the metal in its more favored oxidation state[9].

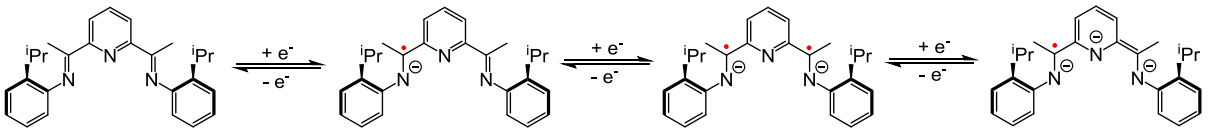

Figure 1.2. Four oxidation states of the PDI complex

Chirik and coworkers show this with their pyridine diamine (PDI, (2,6-ArN=C(Me))$_2$ C_5H_3N) complexes, which is stable in four oxidation states (Figure 1.2). These complexes have been used for hydrogenation and hydro-silylation of olefins, and the cyclization of enynes and dienes. The catalyst used is formally Fe^0 with a neutral ligand. However, further spectroscopic techniques and DFT calculations found that the iron center is actually in the 2+ oxidation state, and the ligand has been reduced by 2 electrons[1]. When cyclizing dienes, the substrate oxidatively adds to the iron center, but the oxidation of that center does not change. Instead, the electrons are pulled from the ligand where they were

Scheme 1.2. PDI Ligand as Electron Reservoir in Fe-Catalyzed [2+2]-Cycloaddition Ring-Closure Reactions

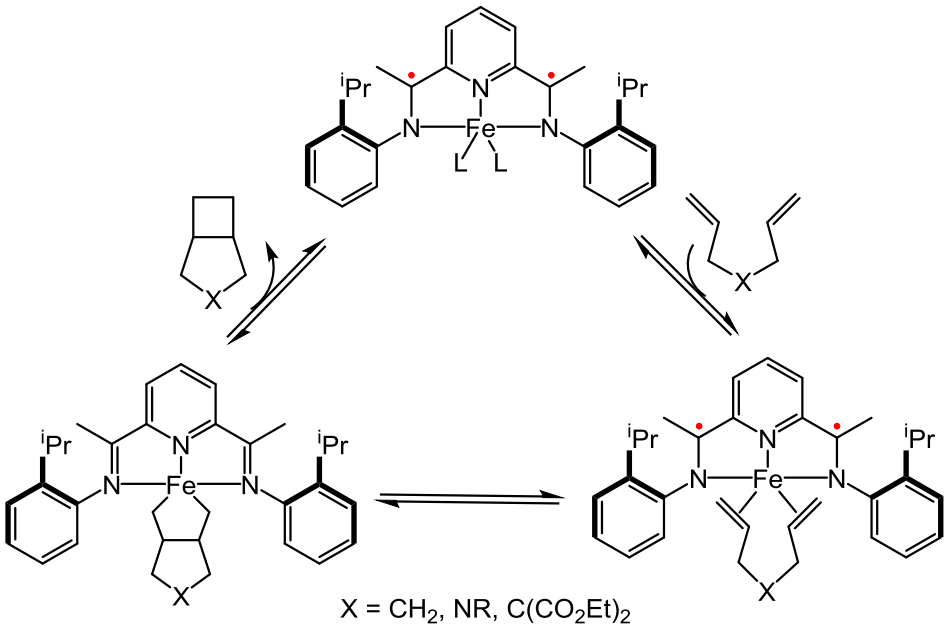

stored, shown in Scheme 1.2. The iron remains in its 2+ state throughout the whole process, but the ligand is the one participating in the oxidation and reductions[9].

This electron storage can go so far as to allow d^0 complexes to participate in catalytic cycles. Heyduk, *et. al.* used the 4,6-di-^{t}butyl-2-^{t}butyl-amidophenolate ligand ($^{t\text{Bu}}$ON) to create d^0 Zr complexes. This ligand has three oxidation states: the fully reduced, dianionic catecholate ($^{t\text{Bu}}NO^{cat})^{2-}$, monoanionic semiquinonate ($^{t\text{Bu}}NO^{sq})^{-}$, and neutral iminoquinone ($^{t\text{Bu}}NO^{q}$). They found that during oxidative addition of X_2 (X = Cl, Br), the ligands lost two electrons, going from $(^{t\text{Bu}}NO^{cat})_2Zr(THF)_2$ to $(^{t\text{Bu}}NO^{sq})_2ZrX_2$ (Scheme 1.3), and that during reductive elimination of Ph_2, the complex went from $(^{t\text{Bu}}NO^{sq})_2ZrPh_2$ back to $(^{t\text{Bu}}NO^{cat})_2Zr(THF)_2$. Again, all of the oxidizing and reduction potential came from the ligand, not the metal. After finding that the bidentate tended to be labile enough in the fully oxidized form to not stay coordinate, they switched to planar tridentate ligands and found that they are capable of group transfer catalysis while utilizing the same principle of electron storage in the ligand[3].

Scheme 1.3. Oxidative Addition of Halogens to $(^{t\text{Bu}}ON^{cat})_2Zr(THF)_2$

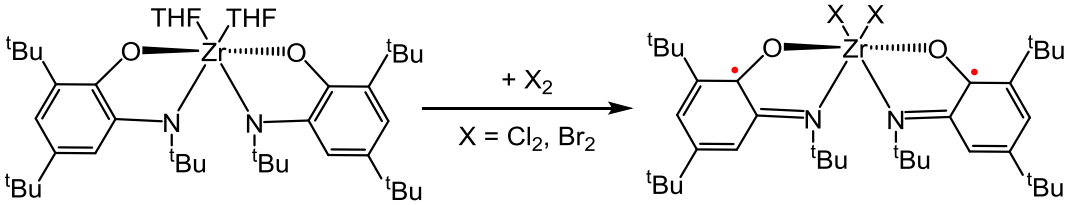

As mentioned before, complexes containing redox-active ligands can form ligand-based radicals. These radicals can directly react with substrates to make and break bonds, while leaving the metal center untouched. Chaudhuri *et. al.* demonstrate this in a biologically-inspired setting, by studying a model for galactose oxidase, which catalyzes aerobic oxidation of primary alcohols to aldehydes and hydrogen peroxide (Scheme 1.4).

They synthesized a dimeric copper thiophenol complex which could not only oxidize primary alcohols to aldehydes, but also couple secondary alcohols together. Once the alcohols bind to the copper centers, the oxygen radicals can abstract the hydrogen off each alcohol, and they are held close enough that they recombine with each other to form the diol. Throughout the process, the only role copper has is to hold the alcohol molecules in place; the ligand is playing the active role of making the bond[10].

Scheme 1.4. Copper-Catalyzed Dimerization of Secondary Alcohols

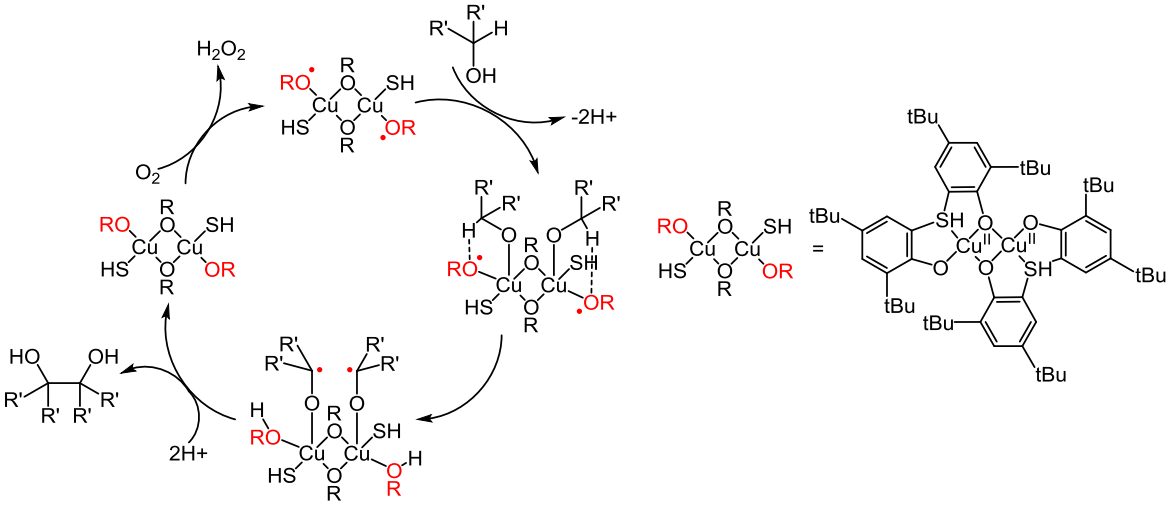

In a related vein, the redox-active, radical-forming "ligand" can be the substrate in order to complete the transformation. This is seen in Co^{II} porphyrin catalyzed nitrene and carbene transfer. When an organic azide or diazo compound reacts with the catalyst, it eliminates N_2 and forms a ligand (substrate) centered radical, shown in Scheme 1.5. In the case of the nitrene, the ligand-based radical can perform an H-atom abstraction, and collapse to form benzylic amines[11] (Scheme 1.5, left). In the case of the carbene, the ligand can react to shift the radical to the coupling alkene, which can collapse to form a cyclopropane[12] (Scheme 1.5, right).

Scheme 1.5. Reactive Substrate-Based Radical Ligands in Nitrene and Carbene Transfer Reactions

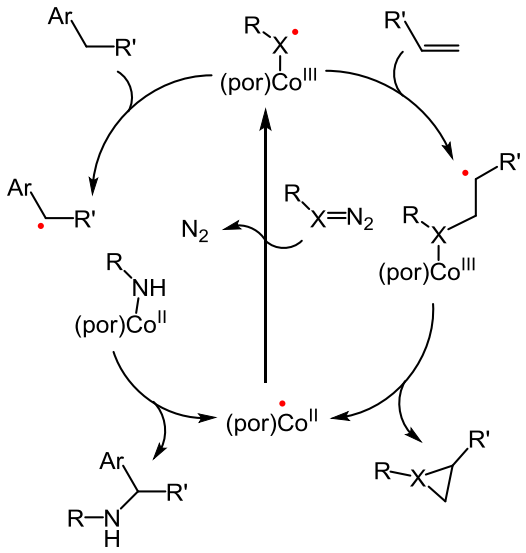

X = N, CH; R = SO_2R, COOR

Oxidation Using 1st Row Transition Metals and Redox-Active Ligands.

Redox-active ligands have been utilized for a wide variety of catalytic transformations, including oxidations. Some of the earliest ligand scaffolds for these reactions were tetradentate ligands, such as porphyrin, corrole, and salen (Figure 1.3). These families of ligands were used because when coordinated to transition metals, they were biomimetic of cytochrome P450 for a variety of oxygen-atom transfer reactions[13, 14]. Other advantages to using these ligands were their open coordination site, where an oxidant could bind, and the ability to generate a high-valent metal-oxo species when one does. However, there are several drawbacks to using these tetradentate ligand systems. The first is that they reversibly form an inert metal-μ-oxo complexes, which limits reactivity[15]. The

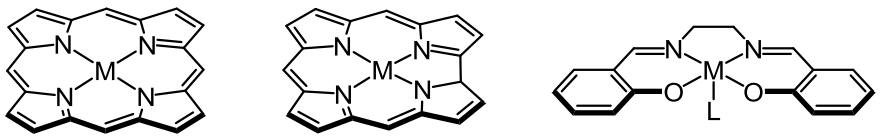

Porphyrin Corrole Salen

Figure 1.3. Examples of tetradentate ligand complexes that offer an open coordination site.

second drawback is that these complexes exhibit product inhibition, where the oxidized substrate irreversibly coordinates to the catalyst (Scheme 1.6). These issues make these systems inefficient, and subsequently produces low turnover numbers (TON).

Scheme1. 6. General Mechanism for Metal-μ-oxo Formation and Product Inhibition

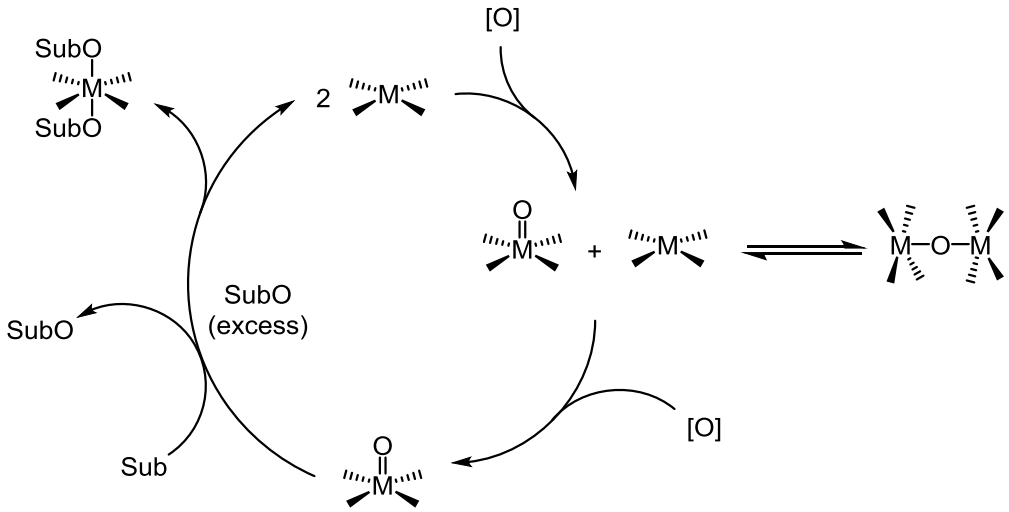

One strategy used to circumvent the previously-mentioned problems is using tridentate pincer ligands instead of tetradentate. While a tridentate pincer ligand has an additional coordination site compared to the tetradentate ligands, which could allow the coordination of another oxidized substrate, a strong *trans* effect weakens the ligation. This *trans* effect also allows any metal-μ-oxo species to dissociate more readily[16]. Because of this, pincer ligand complexes were good candidates for catalytic oxidation reactions.

In the MacBeth group, tridentate NNN pincer ligands are being investigated for use in oxidation and group transfer catalysis with 1st row transition metals. The ligand was designed so the N-amidate donors can stabilize higher oxidation states, due to their strong σ-donor capacity, and are known to be robust under oxidative conditions. A family of ligands were synthesized (Figure 1.4A), but the H_3L^{iPr} will be focused on. The H_3L^{iPr} ligand could be deprotonated and metallated to yield either $[\mathbf{1}]^{2-}$ or $[\mathbf{2}]^{2-}$, depending on the ratio of the starting materials used (Figure 1.4B). $[\mathbf{1}]^{2-}$ was found to have an S=3/2, and three

reversible oxidation events. Two of these events corresponded to one electron, and the third event corresponded to two electrons; some of the oxidations were speculated to be ligand-based. [**2**]$^{2-}$, on the other hand, had several irreversible oxidation events that could not be assigned.

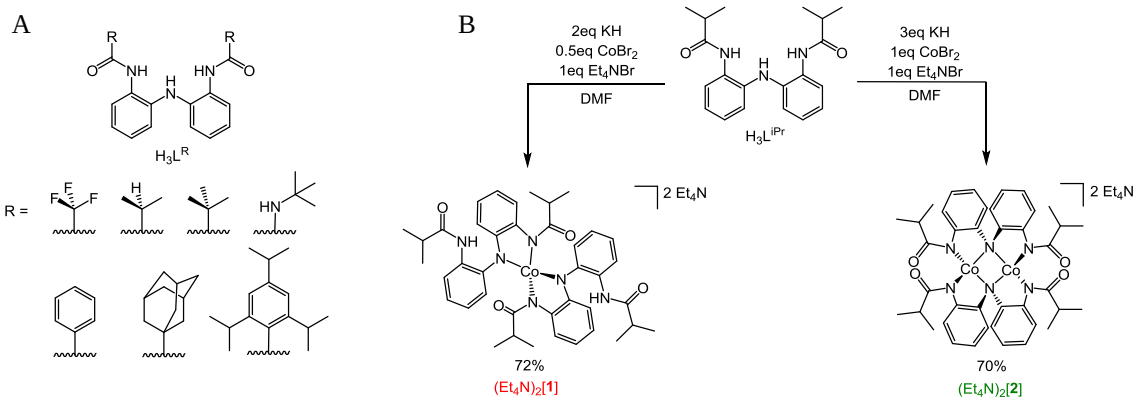

Figure 1.4. (A) Bis(amidophenyl)amine ligands, H_3L^R. (B) Co-monomer and -dimer complex synthesis.

Both cobalt complexes are competent at oxidative and group transfer catalysis. When it comes O-atom transfers, both catalysts could oxidize PPh_3 to PPh_3=O. At 1% catalyst loading and after 2 hours, [**1**]$^{2-}$ had a 69% conversion and a turnover number (TON) = 185, and [**2**]$^{2-}$ had a 95% conversion and a TON = 345. While PPh_3 is not a particularly hard species to oxidize, it has only been done aerobically with 2nd and 3rd row transition metals in the past. In addition, the efficiency of this 1st row metal catalyst was outperforming its noble metal counterparts (TOF > 60 h^{-1}). The complexes were also able to act as a dioxygenase, transferring both oxygen atoms from O_2 to PPh_3[17].

Further investigation went into these complexes, as it was speculated that both monomeric and dimeric species could be going through similar or the same intermediates, indicated by the ~2x TON increase when the cobalt loading doubles. The group found that after O_2 or CN^- was added to either [**1**]$^{2-}$ or [**2**]$^{2-}$, the complexes rearranged to form [**3**]$^-$ and [**4**]$^{2-}$, respectively (Scheme 1.7). [**4**]$^{2-}$ had a spin on 3/2, indicative of Co retains its high

spin. However, [**3**]$^-$ had a spin of 1/2, hinting at a change to low-spin, which is strange for a weaker field O_2^- complex. DFT calculations were used to elucidate the electronic structure of the complex, revealing that the cobalt center has a spin = 3/2, but that there were two radicals: one on the superoxide, and one on the ligand, that both antiferromagnetically couple to the metal center[18].

Scheme 1.7. Formation of [3]$^-$ and [4]$^{2-}$ via Ligand Rearrangement

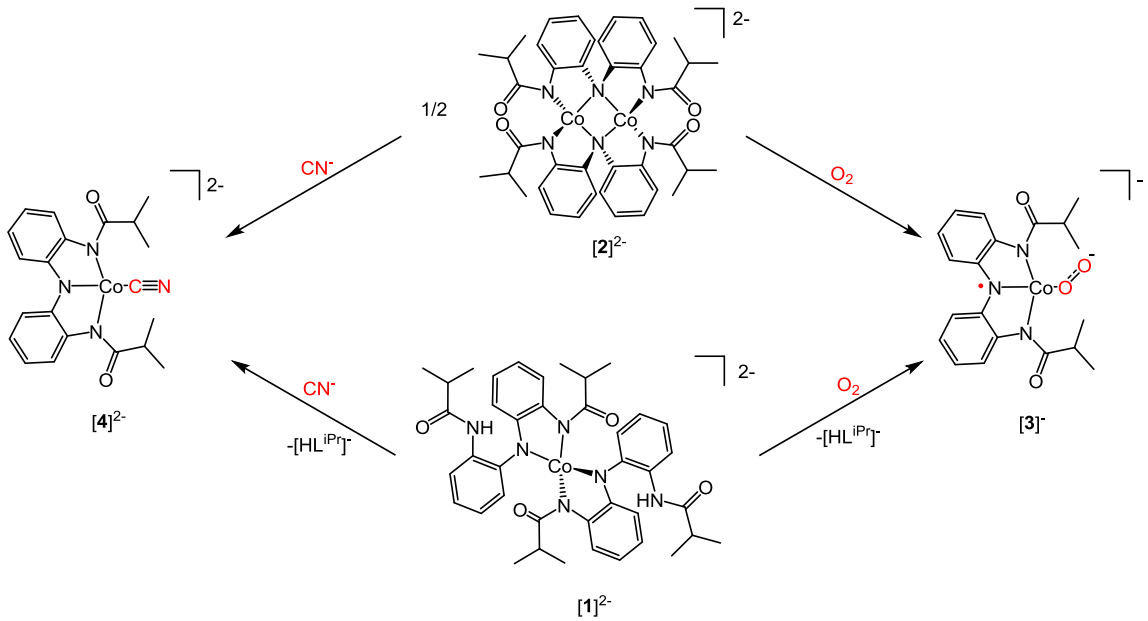

In addition to O-atom transfer, [**2**]$^{2-}$ could catalyze intramolecular C-H amination using aryl and alkyl azides, which has applications in natural products and pharmaceuticals. The reaction was found to be relatively robust, as it was not affected by the resulting ring size, the appearance of pyridine moieties, and a variety of electronic substituents[19]. [**2**]$^{2-}$ could also perform deformylation of 2-phenyl-propionaldehyde, forming acetophenone in good yields. This synthetic catalyst was unique in that only biological systems could carry out aerobic deformylation[18].

References

[1] Chirik, P. J.; Wieghardt, K. *Science*. **2010**, *327*, 794.

[2] Lyaskovskyy, V.; Bruin, B. D. *ACS Catal*. **2012**, *43* (15), 270.

[3] Munhá, R. F.; Zarkesh, R. A.; Heyduk, A. F. *Dalton Trans.* **2013**, *42* (11), 3751.

[4] Schrauzer, G. N.; Mayweg, V. *J. Am. Chem. Soc.* **1962**, *84*, 3221.

[5] Billig, W.; Williams, R.; Bernal, I.; Waters, J. H.; Gray, H. B. *Inorg. Chem.*, **1964**, 3 (5), 663.

[6] Davison, A.; Edelstein, N.; Holm, R. H.; Maki, A. H. *Inorg. Chem.* **1963**, *2*, 1227.

[7] Ringenberg, M. R.; Kokatam, S. L.; Heiden, Z. M.; Rauchfuss, T. B. *J. Am. Chem. Soc*. **2008**, *130*, 788.

[8] Lorkovic, I. M.; Duff, R. R. Jr.; Wrighton, M. S. *J. Am. Chem. Soc*. **1995**, *117*, 3617.

[9] Bouwkamp, M. W.; Bowman, A. C.; Lobkovsky, E; Chirik, P. J. *J. Am. Chem. Soc*. **2006**, *128*, 133340.

[10] Chaudhuri, P.; Hess, M.; Flörke, U.; Wieghardt, K. *Angew. Chem., Int. Ed*. **1998**, *37*, 2217.

[11] Lyaskovskyy, V.; Suarez, A. I. O.; Lu, H.; Jiang, H.; Zhang, X. P.; Bruin, B. D. *J. Am. Chem. Soc.* **2011**, *133*, 12264.

[12] Lu, H.; Dzik, W. I.; Xu, X.; Wojtas, L.; de Bruin, B.; Zhang, X. P. *J. Am. Chem. Soc.* **2011**, *133*, 8518.

[13] Murahashi, S.-I.; Zhang, D., Chem Soc Rev. 2008, 37 (8), 1490.

[14] Meunier, B.; de Visser, S. P.; Shaik, S., Chem Rev. 2004, 104 (9), 3947.

[15] Momenteau, M.; Reed, C. A., *Chem Rev.* **1994,** *94* (3), 659.

[16] O'Reilly, M. E.; Del Castillo, T. J.; Falkowski, J. M.; Ramachandran, V.; Pati, M.; Correia, M. C.; Abboud, K. A.; Dalal, N. S.; Richardson, D. E.; Veige, A. S., *J. Am. Chem. Soc.* **2011**, *133* (34), 13661.

[17] Sharma, S. K.; May, P. S.; Jones, M. B.; Lense, S.; Handcastle, K. I.; MacBeth, C. E. *Chem. Commun.* **2011**, *47*, 1827.

[18] Corcos, A. R.; Villanueva, O.; Walroth, R. C.; Sharma, S. K.; Bacsa, J.; Lancaster, K. M.; MacBeth, C. E.; Berry, J. F. *J. Am. Chem. Soc.* **2016**, *138*, 1796.

[19] Villanueva, O.; Weldy, N. M.; Blakey, S. B.; MacBeth, C. E. *Chem. Sci.* **2015**, *6*, 6672.

Chapter 2 Incorporation of Hydrogen Bond Donors into the Ligand Backbone

Introduction

It is well established that the primary coordination sphere can change the properties of a metal complex. However, the secondary coordination sphere can be of equal or greater importance when it comes to small molecule activation. This is clearly seen in biological proteins with M-O_2, M=O, and M-OH motifs. Metalloproteins such as hemoglobin, cytochrome P450, and horseradish peroxidase all rely on hydrogen bonding to function properly[1].

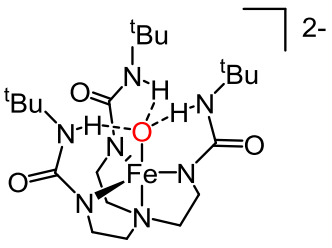

Figure 2.1. $[Fe^{III}H_3buea(O)]^{2-}$

Charged cavities that employ hydrogen bonding are known to stabilize small molecules that would not ordinarily be able to do. Borovik *et. al.* created tripodal ligands that also incorporated second sphere hydrogen bonding in order to activate O_2 (Figure 2.1). The α'NH on the urea groups create a partially positively charged cavity that can form up to three H-bonds with other ligands (eg. OH^-, O^{2-})[1,2]. Fe^{II} and Mn^{II} complexes of $[H_3buea]^{3-}$ were able to produce monomers of the M^{III}–oxo complexes from the activation of O_2. Typically, oxo-ligands consist of a combination of σ- and π-bonds. However, in the cases of $[Fe^{III}H_3buea(O)]^{2-}$ and $[Mn^{III}H_3buea(O)]^{2-}$, the interaction between the oxygen and metal center was characterized as only a single bond. The three H-bonds from the NH groups are strong enough to compensate for the lost π-bond and stabilize the M^{III}-oxido complexes. $[Fe^{III}H_3buea(O)]^{2-}$ and $[Mn^{III}H_3buea(O)]^{2-}$ can then be oxidized to form high-spin $[Fe^{IV}=O]$ and $[Mn^{V}=O]$ complexes, respectively[3]. Similar results were found for $[Co^{III}$-OH] complexes, where the H-bonding from the H_3buea ligand was able to stabilize cobalt's high oxidation state long enough to isolate crystalline solid[4].

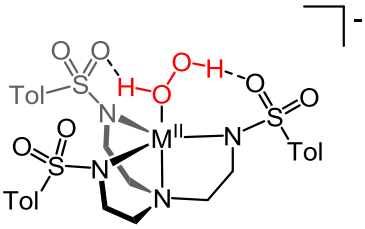

Figure 2.2. Hydrogen peroxide complex of M, where M = Co^{II}, Ni^{II}, Cu^{II}, or Zn^{II}

By switching from a urea-substituted ligand (where α'NH is a hydrogen bond donor) in Borovik's [$M^{II}H_3$buea] complexes to a tosyl-substituted ligand (where oxygen is a hydrogen bond acceptor), small molecules such as water and ammonia can be stabilized instead. This was demonstrated by the Scarborough group, by synthesizing and characterizing hydrogen peroxide complexes of zinc, cobalt, nickel, and copper (Figure 2.2)[5,6]. They found that H_2O_2 binding strength and lifetime were affected by the metal ion used, ligand electronics, and counterion used. Both Borovik's and Scarborough's complexes could ultimately be used to study how hydrogen bonding plays a role in biological systems, such as monooxygenases, the oxygen evolving complex, and Cytochrome P450. They can be used in exploring new oxidation chemistry, using O_2 or H_2O_2 as the terminal oxidant.

Results and Discussion

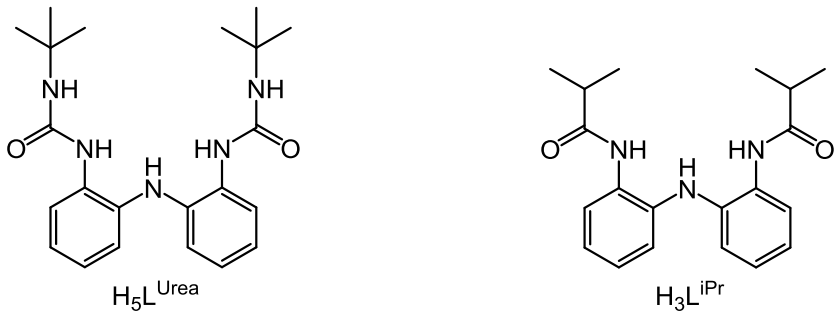

Figure 2.3. H_5L^{Urea} (left) and H_3L^{iPr} (right) ligands

The H_5L^{Urea} ligand scaffold (Figure 2.3, left) was developed with the goal of incorporating hydrogen bond donors into the ligand, with hopes of being able to interact with small molecules such as O_2 once ligated to a metal ion. We predicted that upon

addition of O_2 to these complexes, they would undergo rearrangement similar to previously reported $[\mathbf{1}]^{2-}$ and $[\mathbf{2}]^{2-}$, which used the H_3L^{iPr} ligand (Figure 2.3, right), and form the analogous oxygenated species. It was anticipated that this expected species would be more stable than $[\mathbf{3}]^-$ due to the hydrogen bond donors on the ligand (Scheme 2.1).

Scheme 2.1. Expected Result from Oxidation of H_5L^{Urea} Complexes $[5]^{2-}$ and $[6]^{2-}$

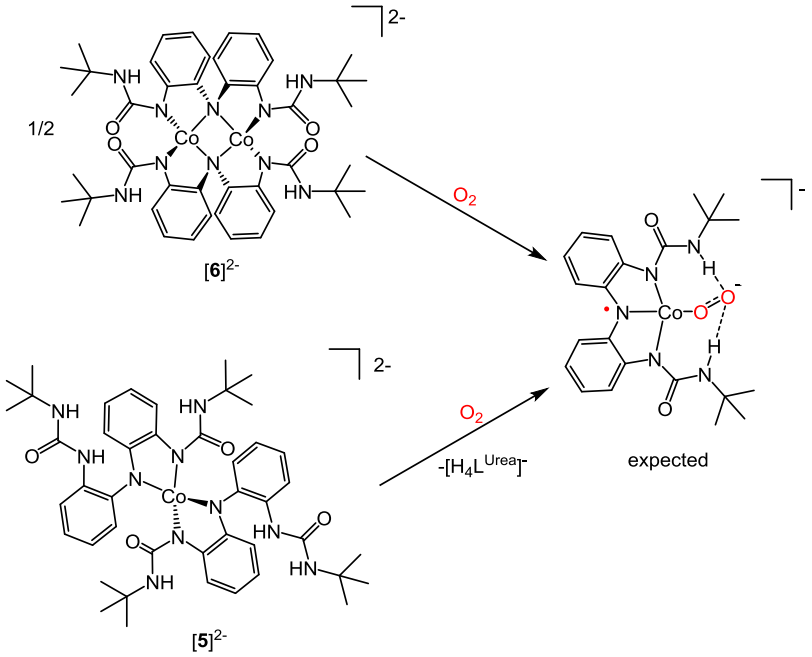

Synthesis of ligand scaffold H_5L^{Urea} was carried out in three steps. HN(*o*-$PhNO_2$)$_2$ was obtained via a nucleophilic aromatic substitution reaction using 2-nitroaniline and 1-fluoro-2-nitrobenzene. HN(*o*-$PhNH_2$)$_2$ was synthesized from the catalytic hydrogenation of HN(*o*-$PhNO_2$)$_2$ using 5 wt% Pd/C. Acylation of HN(*o*-$PhNH_2$)$_2$ with *tert*-butyl isocyanate yields the H_5L^{Urea} ligand as an air-stable white solid in good yield (94%) (Scheme 2.2).

Complexes $(PPh_4)_2$[**5**] and $(PPh_4)_2$[**6**] could be synthesized in the same way as their isopropyl-analogues $[\mathbf{1}]^{2-}$ and $[\mathbf{2}]^{2-}$, respectively[7]. Upon the deprotonation of ligand H_5L^{Urea} in dimethylformamide (DMF) with 2 equivalents of potassium hydride (KH),

Scheme 2.2. Ligand synthesis of H_5L^{Urea}

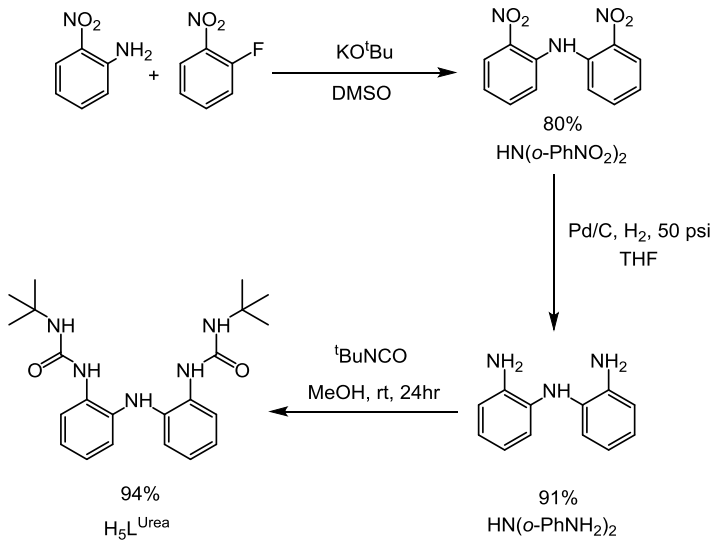

transmetalation with 0.5 equivalents of cobalt (II) bromide ($CoBr_2$), and subsequent *in situ* salt metathesis with tetraphenylphosphonium bromide (PPh_4Br), four-coordinate, mononuclear $(PPh_4)_2$[**5**] was formed in 72% yield. Conversely, when H_5L^{Urea} upon deprotonation in DMF with 3 equivalents of KH, transmetalation with 1 equivalent of $CoBr_2$, and *in situ* salt metathesis PPh_4Br, dinuclear complex $(PPh_4)_2$[**6**] was formed in 18% yield (Scheme 2.3).

Scheme 2.3. Complex synthesis of $(PPh_4)_2$[5] and $(PPh_4)_2$[6]

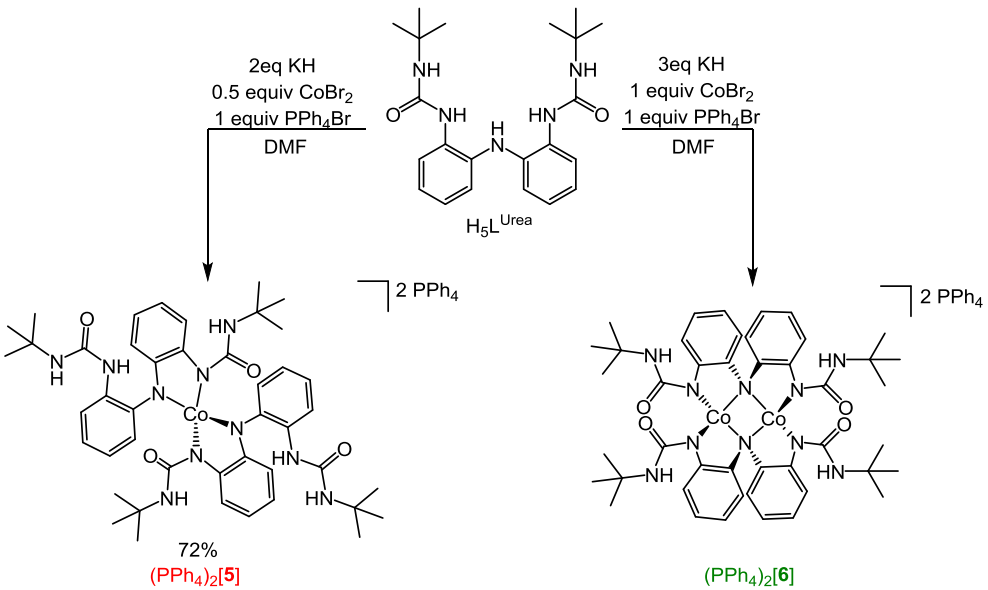

The molecular structures of $[\mathbf{5}]^{2-}$ and $[\mathbf{6}]^{2-}$ were determined by X-ray diffraction (Figure 2.4). Selected bond lengths are given in Table 1. The geometries around the cobalt centers of $[\mathbf{5}]^{2-}$ and $[\mathbf{6}]^{2-}$ differ somewhat from those of $[\mathbf{1}]^{2-}$ and $[\mathbf{2}]^{2-}$. The τ_4 value, described by Houser *et. al.*, is a parameter to describe four coordinate geometries based on a 0.0 – 1.00 scale, where 0.0 is described as an ideal square planar geometry, and 1.00 is an idealized tetrahedral geometry. τ_4 values that fall within this range are typically described as trigonal pyramidal, distorted tetrahedral, or seesaw geometries[8]. $[\mathbf{5}]^{2-}$ has a $\tau_4$of 0.89, while $[\mathbf{1}]^{2-}$ has a τ_4 of 0.80, meaning that while both cobalt centers are distorted trigonal pyramidal, $[\mathbf{5}]^{2-}$ distorts more towards a tetrahedral geometry, while $[\mathbf{1}]^{2-}$ distorts more towards see-saw. $[\mathbf{6}]^{2-}$ is very similar in geometry to $[\mathbf{5}]^{2-}$ around each cobalt center, having a τ_4 of 0.90, while $[\mathbf{2}]^{2-}$ is exactly trigonal pyramidal with a τ_4 of 0.85.

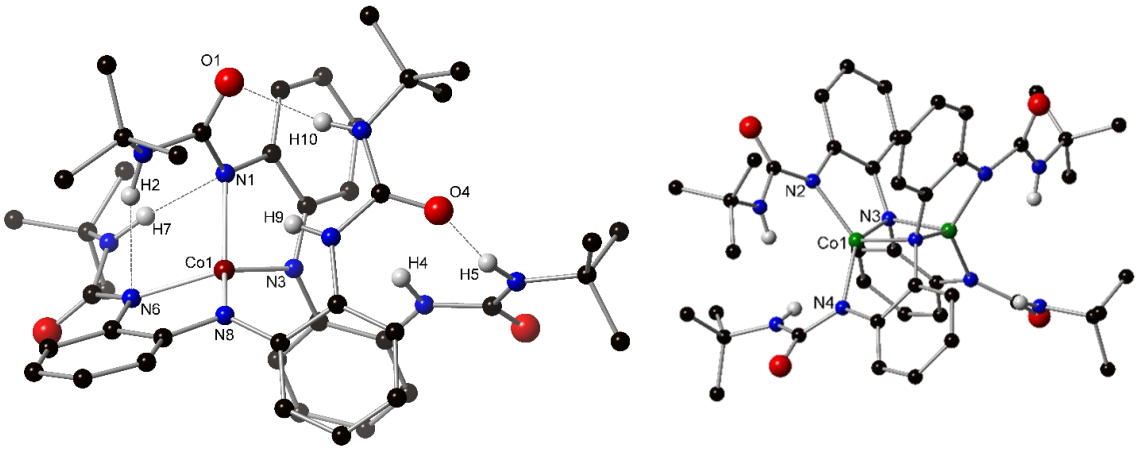

Figure 2.4. Crystal structures of $(PPh_4)_2[\mathbf{5}]$ (left) and $(PPh_4)_2[\mathbf{6}]$ (right) (all hydrogens except for those on nitrogen omitted for clarity). Hydrogen bonding indicated by dashed lines.

Differences between $[\mathbf{5}]^{2-}$ and $[\mathbf{1}]^{2-}$ include slightly shorter Co─N bond lengths (0.032 Å on average), and drastically shorter Co···(N)H distances. The closest four hydrogens are, on average, 0.964 Å closer to the cobalt center in $[\mathbf{5}]^{2-}$ than in $[\mathbf{1}]^{2-}$. $[\mathbf{5}]^{2-}$ also

contains hydrogen bonding between the urea hydrogens and carbonyl oxygens, which helps position the hydrogens in close proximity to the cobalt center. [**6**]$^{2-}$ and [**2**]$^{2-}$ have very similar Co─N bond lengths. However, [**6**]$^{2-}$ has Co···(N)H distances of 2.728 and 2.625 Å, while [**2**]$^{2-}$ does not have any nearby amide hydrogens. The cobalt-cobalt through-space separation distance for [**6**]$^{2-}$ is 2.519 Å, 0.162 Å shorter than that of [**2**]$^{2-}$. This helps us visualize how the hydrogen bond donors change the environment around the metal center, and how that might be able to stabilize reactive intermediates in the future.

Table 2.1. Selected Bond Lengths and Distances for [**5**]$^{2-}$ and [**6**]$^{2-}$

Bond/Interaction	Length (Å)	Bond/Interaction	Length (Å)
	[**5**]$^{2-}$		[**6**]$^{2-}$
Co1─N1	1.995	Co1─N2	1.961
Co1─N3	1.956	Co1─N4	1.962
Co1─N6	1.983	Co1─N3	2.017
Co1─N8	1.994	Co1─N3	2.030
Co1···H2	2.611	Co1···H1	2.625
Co1···H4	3.658	Co1···H5	2.728
Co1···H7	2.543		
Co1···H9	2.674		
N6···H2	2.281		
N1···H7	2.305		
O4···H5	1.938		
O1···H10	2.152		

While $(PPh_4)_2$[**5**] can be isolated purely as a crystalline solid, it is in is in equilibrium with $(PPh_4)_2$[**6**] while in solution. The equilibrium lies more in favor of $(PPh_4)_2$[**5**], which can clearly be seen in the paramagnetic ^{1}H NMR spectra (Figure 2.5).

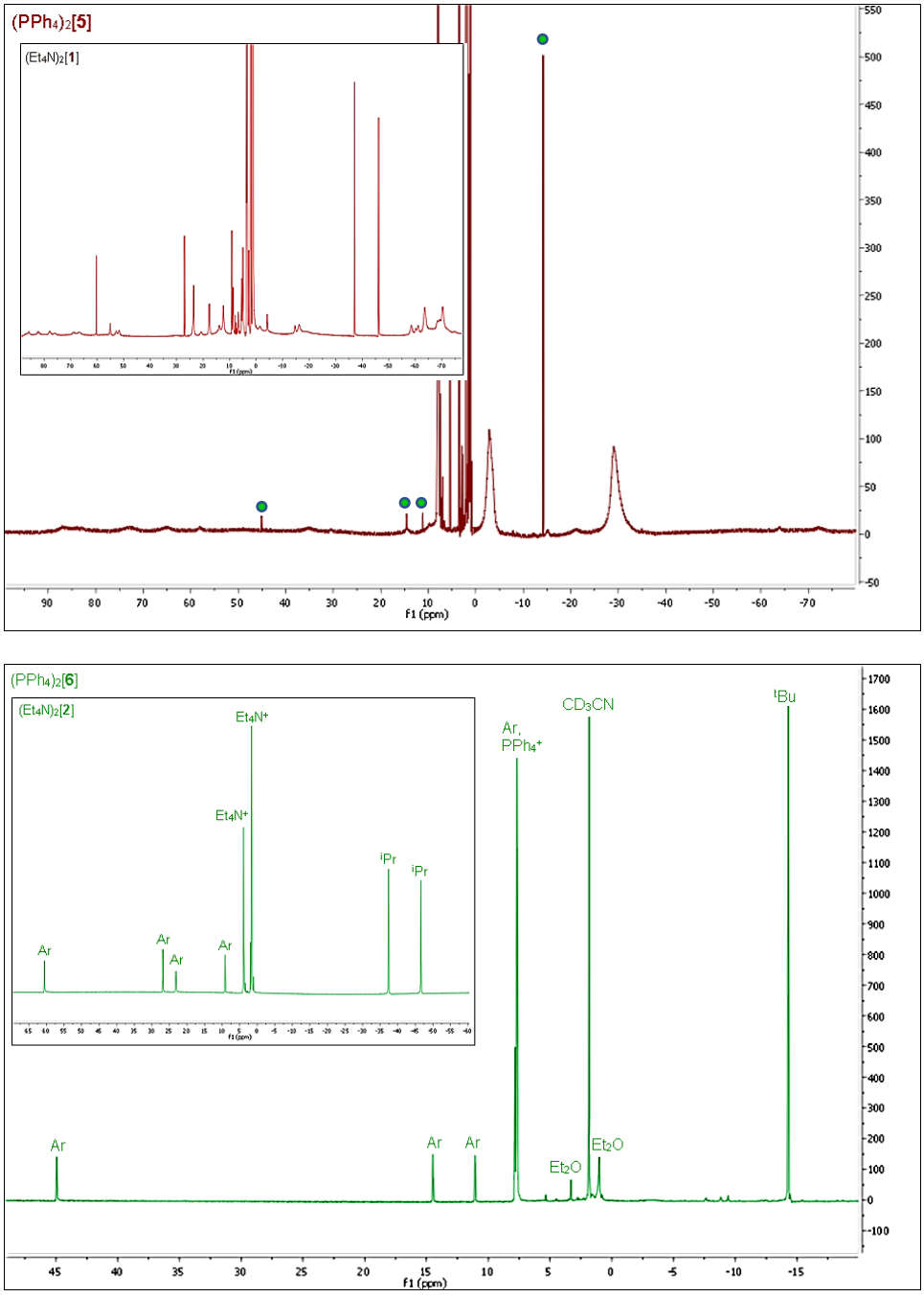

Figure 2.5. Paramagnetic ^{1}H NMR spectra of $(PPh_4)_2$[**5**] (top) and $(PPh_4)_2$[**6**] (bottom). Insets: $(Et_4N)_2$[**1**] (top) and $(Et_4N)_2$[**2**] (bottom). Traces of $(PPh_4)_2$[**6**] labelled with green circles.

The spectrum of $(PPh_4)_2$[**5**] is comprised of many broad peaks due to the asymmetry, proton exchange among the amide protons, and free rotation of the complexed ligand. However, it also contains sharp peaks that correspond $(PPh_4)_2$[**6**], which retains its symmetry and rigidity in solution due to its more fully deprotonated state.

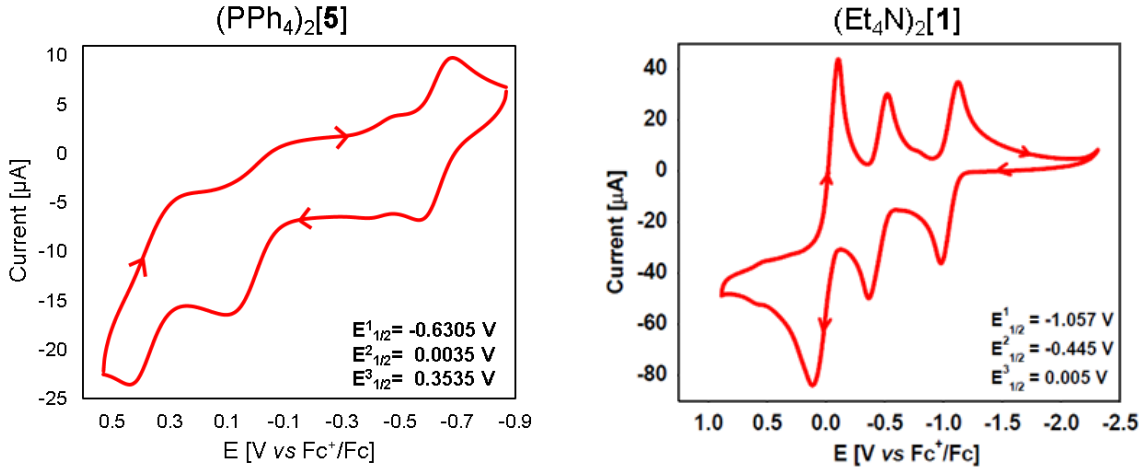

Figure 2.6. Cyclic Voltammetry of $[\mathbf{5}]^{2-}$ (left) compared to $[\mathbf{1}]^{2-}$ (right). Conditions: 100 mV/s. with 0.1 M $TBAPF_6$ in DMF as the supporting electrolyte, referenced vs. Fc/Fc^+, Ag/Ag^+ as the reference electrode, using a glassy carbon working electrode, with scans initially negative.

Cyclic voltammograms were taken of both $[\mathbf{5}]^{2-}$ and $[\mathbf{6}]^{2-}$, and they both showed several electrochemical events. There are broad, unclear events in $[\mathbf{5}]^{2-}$, which further reflects that there is mixture of compounds in solution (Figure 2.6, left). In complex $[\mathbf{1}]^{2-}$ (Figure 2.6, right), the first oxidation event occurs at -1.057 V vs. Fc/Fc^+, suggesting that it readily reacts with dioxygen and undergoes oxidation. In contrast, complex $[\mathbf{5}]^{2-}$ exhibits a quasireversible event at -0.6305 V vs. Fc/Fc^+, which suggests that $[\mathbf{5}]^{2-}$ would be less prone to oxidation under these conditions. Nonetheless, the clear indication of oxidation events in complex $[\mathbf{5}]^{2-}$ seemed to be an indicator that it could accomplish multi-electron chemistry just like its iPr counterpart. However, when tested for catalytic competence by oxidizing PPh_3 to PPh_3O, under the same conditions as previously reported in the group,

$[\mathbf{5}]^{2-}$ could only convert up to 10%. In order to explore what happens to the catalyst in this reaction, $[\mathbf{5}]^{2-}$ was subjected to oxidative conditions in the absence of any substrate, and isolated in order to be characterized. Complex $[\mathbf{5}]^{2-}$ readily reacts with oxygen in a much different way than $[\mathbf{1}]^{2-}$ and $[\mathbf{2}]^{2-}$. In order to synthesize this new complex, 1 equivalent of O_2 was added to $[\mathbf{5}]^{2}$ to form 5-coordinate complex $[\mathbf{7}]^{-}$ (Scheme 2.4).

Scheme 2.4. Oxidation of $(PPh_4)_2[\mathbf{5}]$ to $(PPh_4)[\mathbf{7}]$ using O_2.

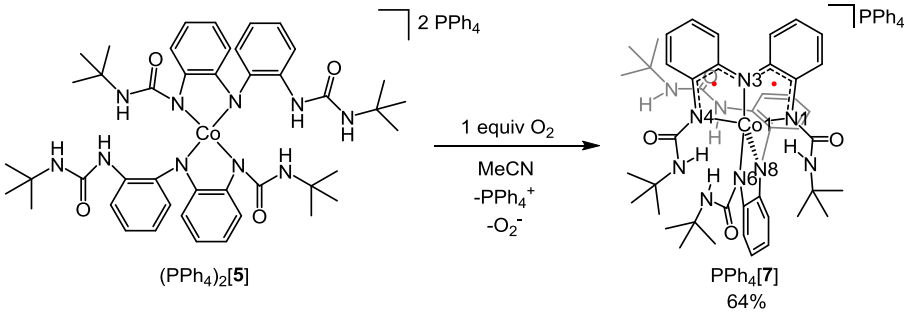

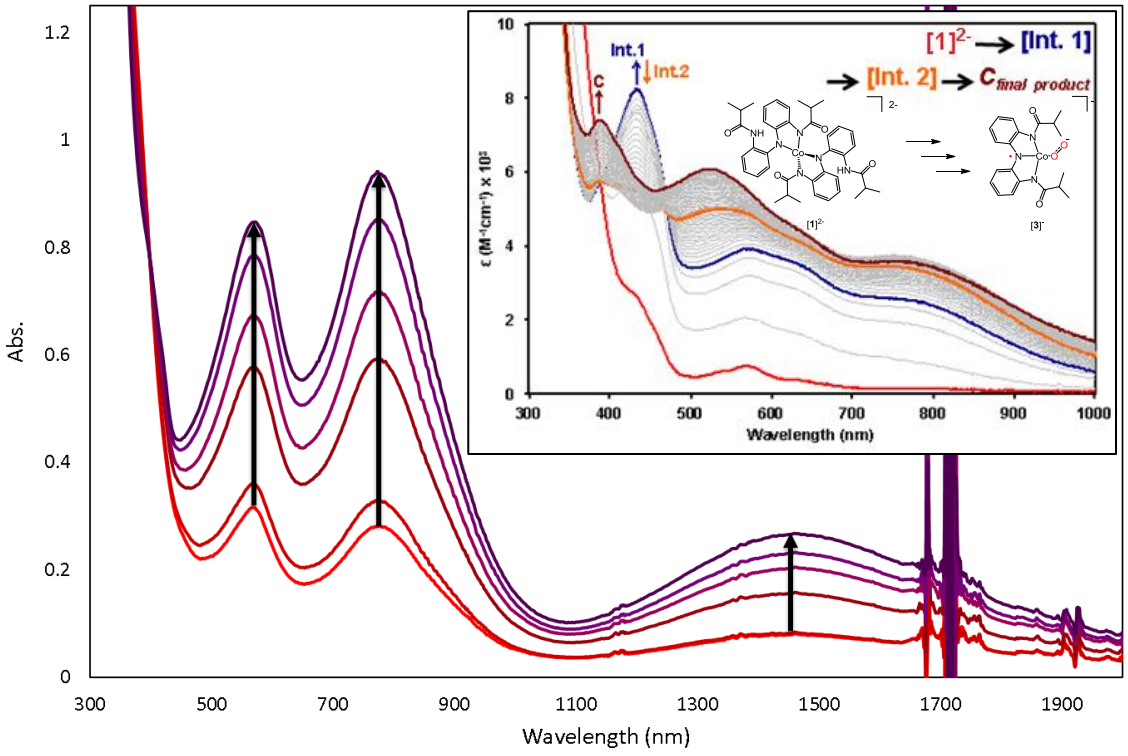

Figure 2.7. 5-minute time lapse electronic absorbance spectrum of the oxidation of $(PPh_4)_2[\mathbf{5}]$ to $(PPh_4)[\mathbf{7}]$. Inset: time lapse electronic absorbance spectrum of the oxidation of $(Et_4N)_2[\mathbf{1}]$ to $(Et_4N)[\mathbf{3}]$.

A time-lapse electronic absorbance spectra was taken of the oxidation of [**5**]$^{2-}$ with O_2. The spectra shows that complex [**5**]$^{2-}$ starts with two d-d transitions at 569 and 777 nm, and that over the course of 5 minutes these bands increase in intensity, and a new peak at 1461 nm appears (Figure 2.7). This new charge transfer band is indicative of radical character in the ligand backbone[9]. It is also worth mentioning that after the oxidized species is formed, it is stable in solution for hours. This again differs from what happens in the conversion of [**1**]$^{2-}$ to [**4**]$^{-}$, where the complex goes through several intermediates before reaching the final product (Figure 6, inset).

A crystal structure of complex [**7**]$^{-}$ was obtained (Figure 2.8), and analysis of the bond lengths further supports the formation of ligand radical character. The crystal structure shows that upon addition of O_2, [**5**]$^{2-}$ is oxidized to 5-coordinate, square pyramidal complex [**7**]$^{-}$. The reason complex [**5**]$^{2-}$ oxidizes to form [**7**]$^{-}$ instead of forming a tridentate species is because of the hydrogen-bonding network that is provided by the urea

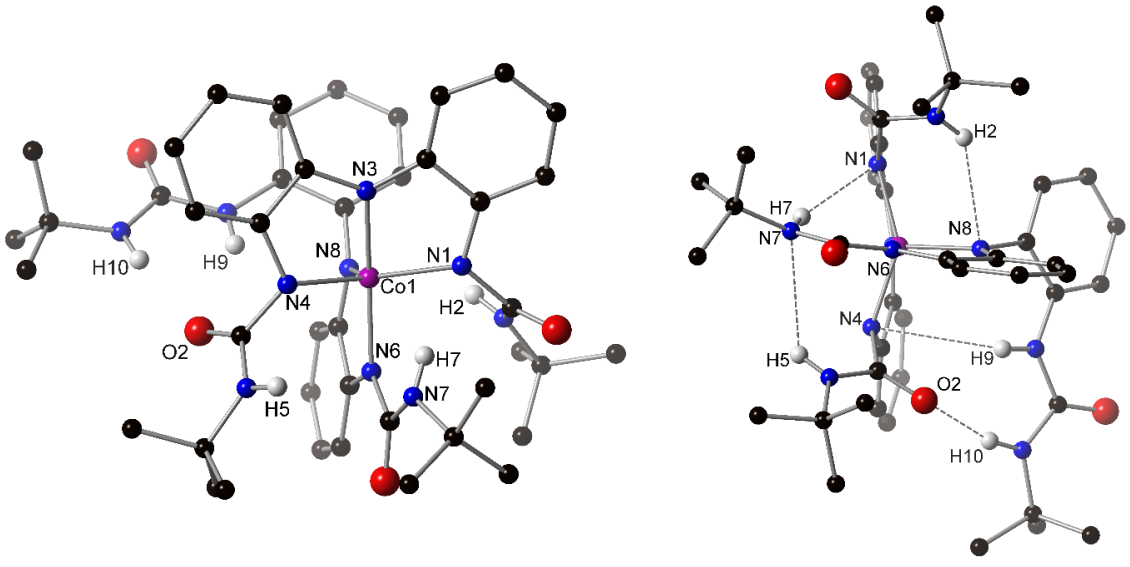

Figure 2.8. Crystal structure of [**7**]$^{-}$ (all hydrogens except for those on nitrogen omitted for clarity). Hydrogen bonding interactions are indicated by dashed lines (right).

Table 2.2. Selected Hydrogen Bonding Distances for [**7**]$^-$

Interaction	Length (Å)
N1···H7	2.431
N4···H9	2.962
N7···H5	2.794
N8···H2	2.601
O2···H10	2.079

substituents on the ligand(Figure 2.8, right). The hydrogen-bonding interactions provide enough attractive forces to stabilize the complex, instead of splitting as it does in the iPr system, which lacks hydrogen-bonding. The Co—N bond length is shorter than that of the Co(II)—N bonds in [**1**]$^{2-}$ and [**5**]$^-$, suggesting a higher oxidation state at the metal center. In addition, the aryl bonds in [**7**]$^-$ alternate between shorter and longer than the reduced complex [**5**]$^{2-}$, indicating localized single and double bond character around the ring, as opposed to when bonds are in resonance and have a more consistent bond length (Figure

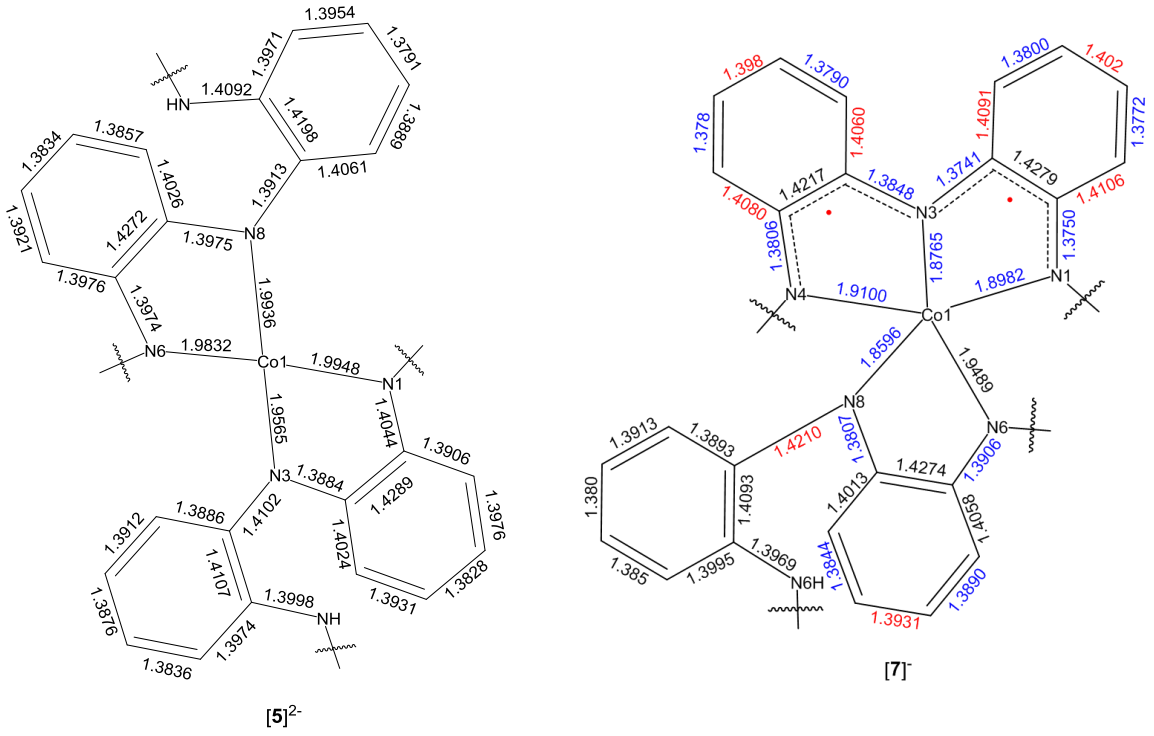

Figure 2.9. Selected bond lengths of [**5**]$^{2-}$ (left) compared to [**7**]$^-$ (right). Bonds lengths in [**7**]$^-$ that are shorter than equivalent bonds in [**5**]$^{2-}$ are shown in blue, and those that are longer are shown in red.

2.9). The localization of single and double bonds is another indicator that there is radical character in the ligand backbone[10].

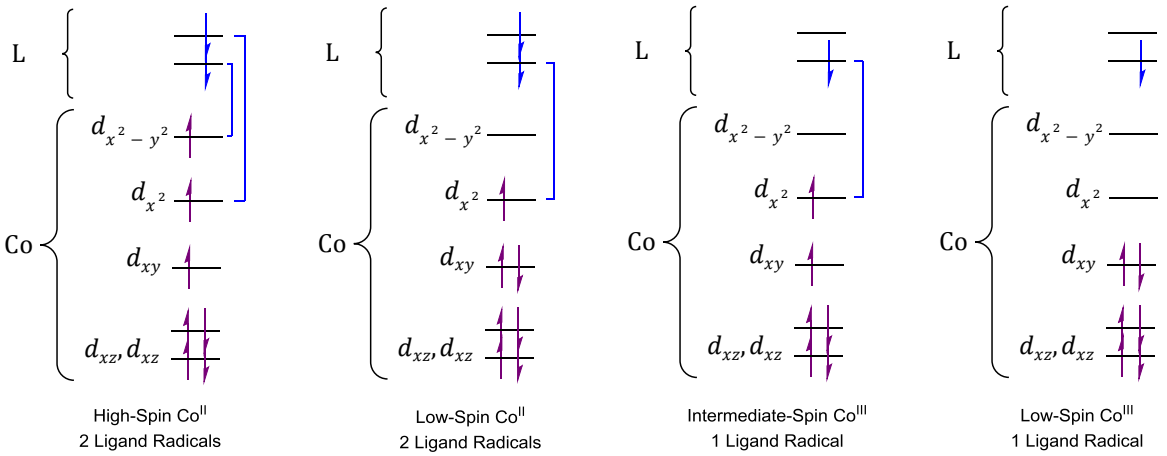

Figure 2.10. Possible electron configurations of [**7**]$^-$.

The magnetic moment of complex [**7**]$^-$ was found to be μ_{eff} = 1.341 μ_B, which corresponds to 1 unpaired electron. Without an XES to elucidate the local spin of the cobalt center, there are four different electron configurations this complex could exhibit, with the possibility of one or two ligand-based radicals (Figure 2.10). The first is where cobalt(II) retains its high spin configuration, and has two electrons antiferromagnetically (AFM) coupled to two ligand radicals, leaving one unpaired electron overall. The second is a low-spin Co^{II} center with one electron AFM coupled to one ligand radical, with a second unpaired ligand radical. The third possibility is an intermediate-spin Co^{III} center, where one electron is AFM coupled to a ligand radical, and the unpaired electron resides in a d orbital. The final option is low-spin Co^{III}, with no AFM coupling, and the ligand radical is the only unpaired electron.

Conclusions

This study describes the synthesis and characterization of Co^{II} complexes supported with H-bond-containing ligand scaffold H_5L^{Urea}, and its reactivity. The H_5L^{Urea} ligand can coordinate to Co monomerically (bidentate) or dimerically (tridentate), identical to the way previous ligand system H_3L^{iPr} did. Electrochemistry shows that both monomeric and dimeric complexes $[\mathbf{5}]^{2-}$ and $[\mathbf{6}]^{2-}$, respectively, undergo multiple events, which initially m ade them good options as oxidation catalysts. It was shown that $[\mathbf{5}]^{2-}$ performed poorly in O-atom transfer compared to $[\mathbf{1}]^{2-}$ and $[\mathbf{2}]^{2-}$, and subsequent isolation of oxidized species $[\mathbf{7}]^{-}$ showed that the hydrogen bonding helped the complex retain two ligands in a 5-coordinate fashion, as opposed to undergoing a ligand rearrangement and forming a tridentate complex with an end-on superoxide. This new complex $[\mathbf{7}]^{-}$ contains one or two ligand-based radicals, supported by UV-Vis/NIR and crystallographic studies.

Future directions pertaining to 2^{nd} sphere hydrogen bonding include finding applications of highly oxidized complex $[\mathbf{7}]^{-}$. The possibility of having 2 ligand-based radicals, lability of the ligands on the potentially high-spin Co center, and open coordination site make it a unique candidate for exploring interesting and relevant oxidations.

Experimental

All manipulations were carried out using standard Schlenk techniques or conducted in a MBraun Labmaster 130 drybox under a nitrogen atmosphere. All reagents used were purchased from commercial vendors and used as received unless otherwise noted. Anhydrous solvents were purchased from Sigma-Aldrich and further purified by sparging with Ar gas followed by passage though activated alumina columns. Oxidized spectra

obtained by injecting stoichiometric O_2 gas into the headspace of the cuvette via a gas-tight, gas transfer syringe

^{1}H NMR spectra were recorded on Varian Mercury 300 and Inova 400 MHz spectrometers at ambient temperature. Chemical shifts were referenced to residual solvent peaks. UV-visible absorption spectra were recorded on a Shimazdu UV-3600 UV-Vis NIR Spectrophotometer using 1.0 cm quartz cuvettes. X-ray diffraction studies were carried out in the X-ray Crystallography Laboratory at Emory University on an XtaLAB Synergy, Dualflex, HyPix diffactometer.

. Cyclic voltammetry experiments were carried out using a CH Instruments (Austin, TX) Model 660C potentiostat. All experiments were conducted in acetonitrile with 0.10 M tetrabutylammonium hexafluorophosphate as the supporting electrolyte. Electrochemical experiments were conducted in a three-component cell consistent of a Pt auxillary electrode , a non-aqueous reference electrode ($Ag/AgNO_3$), and a glassy carbon (CV) working electrode. All electrochemical measurements are referenced and reported versus the ferrocene/ferrocenium couple.

Bis(2-nitrophenyl)amine [HN(*o*-PhNO$_2$)$_2$]. A mixture of 2-nitroaniline (4.0 g, 29 mmol) and 1-fluoro-2-nitrobenzene (3.1 mL, 29 mmol) was stirred in dimethyl sulfoxide (DMSO, 80 mL) at room temperature. KO^{t}Bu (6.5 g, 58 mmol) was added slowly and the reaction stirred under N_2 at room temperature for 24 h. The reaction mixture was then diluted with water (450 mL) and filtered to give a bright orange solid. The solid was recrystallized from MeOH (600 mL) and dried under vacuum to afford the product as a bright orange, crystalline solid (80%, 6.1 g). ^{1}H NMR (δ, $CDCl_3$, 300 MHz): 11.02 (s, 1H), 8.21 (dd, 2H, J = .15), 7.56 (m, 4H), 7.10 (m, 2H).

Bis(2-aminophenyl)amine [HN(*o*-PhNH$_2$)$_2$]. To a tetrahydrofuran (THF) solution of HN(*o*-PhNO$_2$)$_2$ was added 5 wt. % Pd/C. The reaction mixture was placed in a pressure-safe reaction vessel and shaken under H_2 at 50 psi for 45 min. The reaction mixture was filtered through a pad of Celite, and the filtrate was concentrated *in vacuo* to obtain a thick, colorless oil. Crystalline product can be obtained by layering a concentrated diethyl ether (Et_2O) solution of the compound with hexanes (91%, 1.4 g). ^{1}H NMR (δ, $CDCl_3$, 300 MHz): 6.90 (m, 2H), 6.76 (m, 6H), 5.02 (s, 1H), 3.62 (s, 4H).

2,2'-Bis(*tert*-butylamido)diphenylamine (H_5L^{Urea}). To a solution of HN(*o*-PhNH$_2$)$_2$ (1.6 g, 8.1 mmol) in MeOH (30 mL) was added *tert*-butyl isocyanate (1.9 mL, 16.4 mmol). The solution stirred for 18 h at room temperature. The reaction mixture was concentrated in vacuo, and was recrystallized from cold acetone to give a white solid (94%, 3.0 g). ^{1}H H NMR (δ, $CDCl_3$, 300 MHz): 7.63 (m, 2H), 7.48 (s, 2H), 6.92 (m, 4H), 6.73 (m, 2H), 5.58 (s, 2H), 5.35 (s, 1H), 1.31 (s, 18H).

(PPh$_4$)$_2$[Co(H_3L^{Urea})$_2$], (PPh$_4$)$_2$[5]. To a solution of HN(*o*-PhNH$_2$)$_2$ (83 mg, 0.21 mmol) in dimethylformamide (DMF, 10 mL), was added potassium hydride (18 mg, 0.46 mmol). When gas evolution ceased, $CoBr_2$ (14 mg, 0.11 mmol) was added as a solid. When the reaction mixture became homogeneous, tetraphenylphosphonium bromide (88 mg, 0.21 mmol) was added to the red solution. After stirring for 2 h, the DMF was removed under vacuum. The resulting solid was dissolved in a minimal amount of CH_3CN, filtered through a medium porosity frit, and the filtrate was layered with Et_2O to afford dark red crystals. ^{1}H NMR (δ, CD_3CN, 300 MHz): 86.63 (s), 83.62 (s), 72.76 (s), 64.95 (s), 58.10 (s), 45.00 (s), 35.16 (s), 14.33 (s), 11.02 (s), 7.96 (s), 7.84 (s), 5.46 (s), 1.40 (s), -2.80 (s), -14.20 (s), -21.14 (s), -29.26 (s), -63.79 (s), -72.54 (s). λ_{max}, nm (CH_3CN): 569, 777.

$(PPh_4)_2[Co_2(H_2L^{Urea})_2]$, $(PPh_4)_2$[6]. To a solution of $HN(o\text{-}PhNH_2)_2$ (102 mg, .26 mmol) in DMF (10 mL), was added potassium hydride (34 mg, 0.86 mmol). When gas evolution ceased, $CoBr_2$ (34 mg, 0.26 mmol) was added as a solid. When the reaction mixture became homogeneous, tetraphenylphosphonium bromide (109 mg, 0.26 mmol) was added to the green solution. After stirring for 2 h, the DMF was removed under vacuum. The resulting solid was dissolved in a minimal amount of CH_3CN, filtered through a medium porosity frit, and the filtrate was layered with Et_2O to afford dark green crystals (36 mg, 18%). ^1H NMR (δ, CD_3CN, 300 MHz): 45.06 (s), 14.64 (s), 11.19 (s), 7.94 (s), 7.79 (s), -14.19 (s). λ_{max}, nm (CH_3CN): 567, 776.

$(PPh_4)[Co(H_2L^{Urea})(H_3L^{Urea})$, PPh_4[7]. $(PPh_4)_2$[**5**] was loaded into a Schlenk flask and dissolved in CH_3CN. The flask was brought outside of the glovebox, and O_2 gas was added into the headspace via a gas-tight, gas transfer syringe. After an immediate color change from red to dark purple, the reaction solution stirred for an additional 3 hours. The resulting solution was concentrated *in vacuo* and pumped back into the glove box. The residue was washed with diethyl ether, dissolved in CH_3CN, and filtered through a medium porosity frit. The CH_3CN was removed under vacuum, and the product was recrystallized by layering THF with Et_2O. λ_{max}, nm (CH_3CN): 572, 773, 1461.

References

[1] Borovik, A. S. *Acc. Chem. Res*. **2005,** *38*, 54.

[2] MacBeth, C. E., Gupta, R., Mitchell-Koch, K. R., Young, V. G., Lushington, G. H., Thompson, W. H., Hendrich, M. P., Borovik, A. S. *J. Am. Chem. Soc*. **2004**, 126, 2556.

[3] Cook, S. A., Borovik, A. S. *Acc. Chem. Res*. **2015**, *48*, 2407.

[4] Jones, J. R.; Ziller, J. W.; Borovik, A. S. Inorg. Chem., 2017, 56, 1112.

[5] Wallen, C. M., Bacsa, J., Scarborough, C. C. *J. Am. Chem. Soc.*, **2015**, *137* (46),14606.

[6] Wallen, C. M.; Bacsa, J.; Scarborough, C. C. *Inorg. Chem.*, **2017**, *Article ASAP*.

[7] Sharma, S. K.; May, P. S.; Jones, M. B.; Lense, S.; Handcastle, K. I.; MacBeth, C. E. *Chem. Commun.*, **2011**, *47*, 1827.

[8] Yang, L.; Powell, D. R.; Houser, R. P., *Dalton Trans.*, **2007,** *9*, 955.

[9] Dunn, T. J.; Webb, M. I.; Hazin, K.; Verma, P.; Wasinger, E. C.; Shimazaki, Y.; Storr, T. *Dalton Trans.*, **2013**, *42*, 3950.

[10] Chaudhury, P.; Verani, C. N.; Bill, E.; Bothe, E.; Weyhermüller, T.; Wieghardt, K. *J. Am. Chem. Soc.*, **2001**, *123*, 2213.